ORIGINAL ARTICLE

A C G publications

J. Chem. Metrol. 16:2 (2022) 78-89

journal of chemical metrology

Development of chemometrics method based on infrared spectroscopy for the determination of cement composition and process optimization[§]

Dilek Tepeli [1*], Durmuş Özdemir [1] and Mehmet Gökhan Gümüş [2]

[1]*İzmir Institute of Technology Faculty of Science, Chemistry Department, 35430, İzmir, Türkiye*

[2]*BATIÇİM Batı Anadolu Çimento Sanayii A.Ş.,35050 İzmir,Türkiye*

(Received October 11, 2022; Revised November 21, 2022; Accepted December 10, 2022)

Abstract: In combination with a multivariate calibration method, FTIR-ATR spectroscopy was presented as a rapid method for the determination of some major oxides (CaO, SiO_2, Al_2O_3, Fe_2O_3) and minor oxides (MgO, SO_4, Na_2O, and K_2O) in diverse materials (raw material, raw meal, additives, clinker, and types of cement) in cement manufacturing. The FTIR spectroscopy based multivariate models were generated by taking X-ray fluorescence (XRF) as a reference method. Among a number of spectral preprocessing methods, extended multiplicative scatter correction (EMSC) yielded the best PLS models. The standard error of prediction (SEP) for the optimal FTIR based PLS models ranged from 0.10 to 2.07 (w/w%), and the regression coefficient (R^2) ranged from 0.95 to 0.99 for PLS predicted vs XRF reference plots. Statistical evaluation of the both methods was carried out by paired t-test at the 95% confidence level and the results showed that the FTIR-ATR combined with PLS model results are consistent with the XRF reference measurements for all the oxides studied. Compared to the XRF method, which can take anywhere from a few minutes to an hour for each measurement, the proposed method is faster, cheaper, and safer. The presented technology also allows rapid monitoring of a cement factory production line.

Keywords: Cement composition; PLS, oxide determination; FTIR; XRF.

1. Introduction

Cement is produced by mixing raw materials comprising calcium, silicon, aluminum, and iron oxide in a controlled manner. The manufacturing technology of cement is comprised of five main stages. First, crushing and grinding the raw materials such as limestone and clay, and second, blending the raw materials in controlled proportions. Third, clinker production by burning the raw meal at 1450 °C. Four involves grinding the clinker with around 5% calcium sulfate (gypsum) or other additives in appropriate proportions depending on the type of cement produced. The final step is packaging, during which the silo-stored (depending on the kind of cement) products are bagged or delivered to the market in bulk, according

* Corresponding author E-Mail: dilek.tepeli95@gmail.com

[§]This study has also been presented as an oral presentation at 10. National Analytical Chemistry Congress at Muğla Sıtkı Koçman University, Muğla, Türkiye on September 08 – 11, 2022.

The article was published by ACG Publications
http://www.acgpubs.org/journal/journal-of-chemical-metrology July-December 2022 EISSN:1307-6183
DOI:http://doi.org/10.25135/jcm.76.2210.2601
Available online: December 15, 2022

to market demand. The TS EN 197-1 standard classifies cement varieties for general use (CEM type) into five primary types. CEM I-Portland cement, CEM II-Portland composite cement, CEM III-Portland Blast Furnace Slag Cement, CEM IV-Pozzolanic cement, and CEM V- Composite cement. In addition, these primary types encompass a total of 27 sub-varieties of cement [1]. Oxides, including calcium oxide (CaO), silica oxide (SiO_2), aluminum oxide (Al_2O_3), and iron(III) oxide (Fe_2O_3), are the primary ingredients of cement. All stages of cement manufacture are sensitive to variations in the concentration of chemical oxide components resulting in alterations in the quality of materials used in cement production, including the final product. Final product quality is closely related to the oxide ratio of raw materials, raw meals, and additives; therefore, maintaining a steady ratio of ingredients throughout production is essential for a high-quality end product. In cement factories, samples from each step of the production process, including raw materials, raw meal, clinker, gypsum, additives, cement types, and packed end products, are submitted hourly to quality control laboratories for quantitative chemical analysis. On the basis of the quantitative component results of the samples sent from the intermediate production steps, appropriate intervention is initiated in the production line. This means that a significant number of samples are sent daily from the production line to the quality control laboratories, and that the results of these chemical analyses must be obtained quickly and accurately to implement the necessary interventions without slowing down production. Therefore, it is essential to prioritize fast, accurate, low-cost method to optimize manufacturing line, quality control, and product quality. Classical wet chemical methods have been used in past years to quantify cement composition in terms of six essential oxides [2-3]. In response to the limitations of the traditional wet chemical methods, many spectroscopic analysis techniques have been developed for use in identifying cement's chemical components. In this application area, AAS [4,5], ICP [6,7] and XRF [8-10] provide elemental analysis in equivalent oxides for the assessment of cement composition. Also, X-ray diffraction (XRD) is utilized to identify mineral constituents [11,12]. However, the sample preparation for the available techniques is laborious and requires various chemicals and a long time is needed to complete the steps The mentioned techniques cannot meet the need for rapid measurement due to the large number of chemical analyses required during the manufacturing process on an industrial scale. Presently, the majority of cement factories perform quantitative chemical composition analyses of cement by following ASTM C114-15 [2], and in Turkey, the TS EN 196-2 standards [13]. The conventional chemical test methods are specified as reference methods in the ASTM C114 and TS EN 196-2 standards, whereas XRF is indicated as an alternative quick instrumental test method.

Although XRF is faster than other wet chemical methods, sample preparation is crucial to the success of XRF. Sample preparation for XRF measurements must be careful and controlled, and analysis times would range from 15 minutes to an hour, depending on the material being analyzed. When a negative situation, such as the malfunction of an XRF instrument, occurs in a factory, the gadget's repair can take days or even months. XRF instrument is relatively pricey. Additionally, the use of radioactive sources might be a safety concern for users. Considering the disadvantages of XRF and the possibilities that such difficulties can occur, it's important to have a backup analytical approach ready instead of dealing with laborious wet chemistry methods.

In contrast, Infrared spectroscopy has only been utilized in a handful of studies for the quantitative investigation of cement-type materials, but other spectroscopic techniques have been utilized extensively. The contents of that studies are as follows; First, Zaine et al. investigated the carbonate and clay mineral chemistry of cement raw material rock samples using shortwave infrared (SWIR) spectroscopy. Utilizing CaO and Al_2O_3 measurements of portable X-ray fluorescence, the authors evaluated the wavelength location and depth of CO_3 and Al-OH absorption properties. The CaO and Al_2O_3 correlation coefficients for each type of limestone were determined to be 0.774 and 0.842 for dark gray limestone, 0.787 and 0.723 for light gray limestone, and 0.695 and 0.905 for dolomitic limestone [14] . Second, XRF is typically used for cement alkali testing; however, Nasrazadani and Springfield have adapted FTIR for speedier measurements. The quantity of alkali is determined by the analytical absorption band at 750 cm^{-1} in the FTIR spectra of cement samples derived from an Alkali solid solution of tricalcium aluminate C_3A. In the study, pellet creation is employed as a sampling approach in FTIR, which comprises multiple processes (dilution, mixing, milling), and the authors emphasize the necessity for extreme care in pellet making to achieve consistent spectra and results [15]. Third, Near-infrared emission spectroscopy (NIRES) has been studied to determine CaO, SiO_2, Al_2O_3, Fe_2O_3, MgO, and SO_3 in Portland cement samples. A NIRES-

AOTF (Acousto-Optical Tunable Filter) spectrometer was assembled to develop the method. NIRES second derivative spectra were correlated with XRF elemental reference analyses using PLS regression models (XRF). The independent validation set's regression coefficients (R^2) ranged from 0.63 to 0.95. The authors mentioned that no saleable instrument (NIRES-AOTF) is presently available for usage at cement facilities to monitor the production process [16]. In the final study, the combination of near-infrared (NIR) diffuse reflectance spectroscopy and chemometrics were provided as a speedy and accurate method for identifying the major components (CaO, SiO_4, Al_2O_3, and Fe_2O_3) in the cement starting material. Several regression techniques, including partial least square (PLS), interval partial least square (iPLS), and synergy interval PLS (siPLS), in conjunction with several pretreatment methods, were used to examine the correlations between NIR spectra and the X-ray Fluorescence (XRF) reference method. The iPLS technique yielded ideal models with root-mean-square-error-of-prediction (RMSEP) ranging from 0.0379 to 0.1715 and correlation coefficient (Rp) from 0.7294 to 0.9304 [17].

The objective of this research is to develop partial least square calibration models of cement-type materials (raw materials, raw meal, clinker, gypsum, other additives, and types of cement) using FTIR-ATR spectra and XRF for major (CaO, SiO_2, Al_2O_3, Fe_2O_3) and minor (MgO, SO_3, Na_2O K_2O) oxides to control production line. As far as we know, no published study employed the summation of FTIR-ATR spectra of many cement-type materials that include finished cement products and taken directly from a cement plant's production process, to determine major and minor oxides. The study describes an analytical approach that does not require sample preparation, making it practical, fast, and cost-effective.

2. Experimental

2.1. Sample Analyzed

The samples were taken from the BATIÇİM/BATI ANADOLU cement plant in Izmir, Turkey, and collected over a period of one month. The study includes samples generated in the same facility for sale or utilized in producing the final product. The research was comprised 51 samples of cement, including CEM-I, CEM-II, and CEM-IV varieties, along with samples of 20 clinker, 11 limestone, 9 gypsum, 6 raw meal, 5 clay, 5 iron ore, 3 trass, 3 fly-ash.

2.2. Reference Analyzes of the Samples

In the current study, the reference elemental composition of the investigated samples was determined with XRF (Pananalytical axios WDXRF) using two distinct sample preparation techniques, depending on the sample type [13]. The pressed pellet technique was used on samples of cement and clinker, while a glass bead preparation was used on raw materials and additives. Calibration of the XRF instrument for the pressed pellet sampling technique was conducted with Laboratory Test Programme (LTP) samples for each type of material (cement types, clinker). The LTP samples are gathered from the Turkish Cement Manufacturers' Association and analyzed by many laboratories affiliated with the Institution. The z-score value is acquired by each laboratory to show the repeatability of the analyses. For the calibration of each oxide, the mean value of results which is obtained from each laboratory is used. Moreover, CRM samples are utilized to calibrate the XRF instrument for the glass bead sample preparation process. Each type of material which is evaluated using glass bead preparation is calibrated independently for each oxide. The reason for applying two different sample preparation methods to specific types of samples is to minimize the XRF errors that may arise from the particle sizes of the samples. Because the exit particle sizes of the raw materials from the kiln are larger than the intermediate and final output. Although the samples are thinned sufficiently before XRF analysis homogeneity between products cannot be attained. Since the glass bead preparation procedure involves melting the raw material samples between 900 and 1200 ℃, errors caused by particle size can be avoided. As a routine procedure, the quality control laboratories of the manufacturer apply these two processes to the provided samples [18].

2.2.1. Pressed Pellet Technique

The procedure for forming pressed pellets for XRF analysis consists of five significant steps: milling the sample to a fine grain size, weighing it, adding a binder, combining it with a binder in a grinding vessel, and pressing at a constant pressure. The technique is described in detail below.

First, the sample weighed 20 grams. Then, the sample was mixed with the grinding or tableting aid. The amount of grinding aid to be applied varies according to the characteristics of the sample. Then, the sample and tableting aid were reduced to tiny particles using a pulverizer. Small particle size is essential for making pellets yield the best analytical results, as it impacts how the sample compresses and holds when pressed. After the mixture was ground, it was placed into a mixing vessel, and triethanolamine was added as a binder. The mixing vessel was put into the mill's pulverizer. In the mill, the sample and binder were ground together. 5.0 g of the mixture was put into a pressing die and subjected to a steady, predetermined pressure. Finally, the pellet was ready for XRF measurement.

2.2.2. Glass Bead Preparation

Three primary steps are involved in producing glass beads from a sample. First, the sample is mixed with flux. Second, by melting the sample at high temperatures into glass beads. Lastly, a mold can shape a molten mixture into discs. The exact method for producing a glass bead for XRF analysis is detailed below.

The sample was weighed, and the exact amount of tetraborate used as a flux was also weighed. After that, the sample and flux were combined and transferred to a platinum crucible. Calcium iodide was then added to simplify the melting process. The mixture was melted in a platinum crucible at temperatures between 900 to 1200 ℃. While a sample of the mixture was melting, it was being shaken constantly. Using a mold, the molten fluid was shaped into a disc. The resulting glass bead was subsequently analyzed.

The reference results of the samples are given in terms of percentages of oxides measured by XRF in Table S1. (see supporting information)

2.2.3. Loss of Ignition Analysis (LOI)

The quantity of weight lost by raising the temperature of raw material, cement, to a predetermined level is known as ignition loss. The loss of ignition analysis of the samples was carried out according to Turkish standards, TS EN 196-2 [13], with a total of 85 samples. Clinker samples are produced by burning raw meals at high temperatures in the absence of moisture; hence, the loss of ignition analyses (LOI) do not perform in the quality control laboratory of most cement factories. For the LOI parameter, clinker samples were eliminated from the data set.

The reference results of the samples are given in terms of percentages of L.O.I in Table S2. (see supporting information)

2.3. FTIR-ATR Measurements and Data Treatment

The samples were analyzed using a Fourier transform infrared spectrometer (PerkinElmer Spectrum 100 FT-IR) with an attenuated total reflectance (PIKE MIRacle) accessory as a sampling approach without extra sample preparation The spectra were investigated between the wavenumber ranges of 4000 cm^{-1} and 550 cm^{-1}. The optimal resolution was determined to be 8 cm^{-1} (data point interval, 2 cm^{-1}1), and 16 scans were performed. For each sample, measurements were performed in triplicate to minimize spectrum errors resulting from sample particle size. The average spectrum of each sample is given in Figure 1 and was used in multivariate analysis. Importing the FT-ATR-obtained spectra into Microsoft Excel 365, the calibration data set and an independent validation data set were constructed. 89 samples were included in the calibration data set, and the remaining 24 samples were included in the independent validation set. (80% for calibration data set and 20% for validation data set). The data sets were arranged based on the validation and calibration sets contain samples with comparable composition. The validation data set was designed to encompass all sample types.

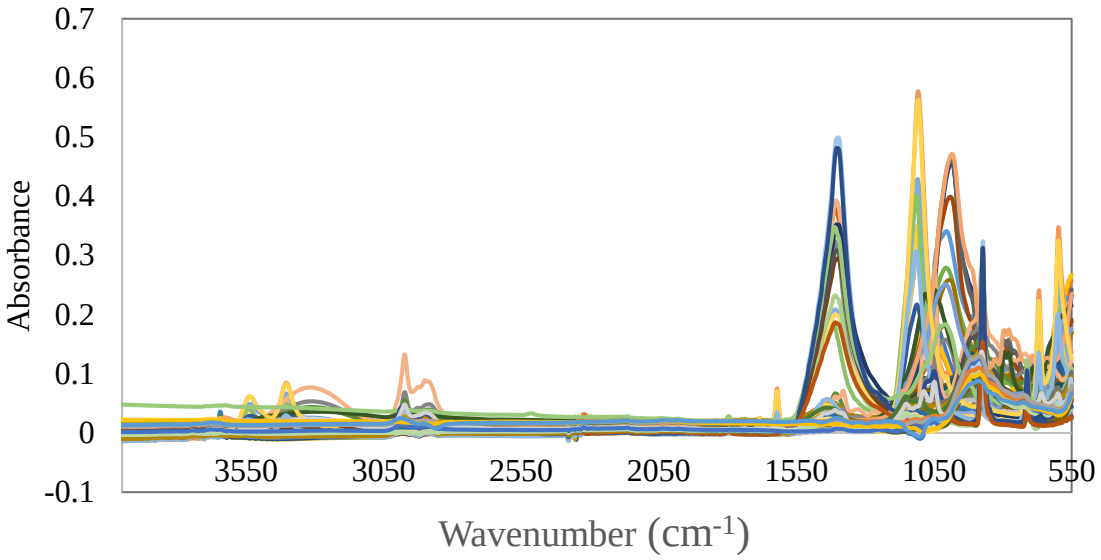

Figure 1. FTIR – ATR spectra of all samples of various cement types, raw materials, and additives

2.4. Pre-Processing and Partial Least Square (PLS)Regression

The obtained spectra may be affected by factors other than oxide concentration, such as the particle size of the sample, the presence of stray and scattered light, and the spectrometer's vibration noise. Using various preprocessing techniques, the impact of these interfering factors can be minimized. The region between 2450–2350 cm^{-1} was excluded from the spectra because it showed absorption caused by the atmospheric carbon dioxide that was irrelevant to oxides before applying any preprocessing. After, multiple preprocessing techniques, including Multiplicative Scatter Correction (MSC) [19], Baseline Correction [20], and Extended Multiplicative Scatter Correction (EMSC) [21,22], were applied to the raw spectra. The Extended Multiplicative Scatter Correction (EMSC) pre-processing approach yielded the best PLS models.

In calibration data modeling, partial least-squares (PLS) is a factor analysis-based technique that minimizes data to reduce spectral and concentration errors. Haaland, Kowalski, and coworkers have elucidated PLS in detail [23,24]. After preprocessing, PLS method was performed to the data to develop calibration models using the chemometrics calibration toolkit 'OBA quantifier' from OBA Kemometri in the MATLAB R2018b environment (Math Works Inc., MA). The full range of spectra was mean-centered and used to construct the PLS models. The Leave-one-out cross-validation pattern was used to determine optimal number of latent variables [25]. Standard error of prediction (SEP) and regression coefficients (R^2) were used to assess the performance of the final PLS model for each oxide.

3. Results and Discussion

After EMSC sample preprocessing, the spectra of all samples are displayed in Figure 1 and utilized to develop PLS models for main and minor oxides. To differentiate between sample types included in the data set, Figure S1 for cement types, Figure S2 for clinker, Figure S3 for additives, and Figure S4 for raw materials display the sample spectrum for each type. (See supporting information.) There are noticeable spectrum variances between these types, reflecting their distinct sample compositions and establishing the foundation for effective PLS regression on the FTIR-ATR spectra. Qualitative interpretation of cement-type materials is performed in detail in the Mid-range (400-4000 cm^{-1}) by Hughes et al. [26]. Concentration data is required for PLS model construction. Sample concentrations obtained by XRF spectrometer serve as a reference, and those values are listed in Table S1 for each oxide. (See supporting information.) During validation, the concentrations of the oxides in the independent set covered the whole range, indicating that the samples were correctly distributed. For the first 30 LVs, the optimum number of latent variables for each oxide was identified by calculating the predicted residuals

errors sum of squares (PRESS) using cross-validation with mean-centering. The correlation performance is then determined by plotting the predicted oxide (w/w%) values against the XRF reference oxide (w/w%) values. Following the construction of temporary PLS models, outlier detection is performed based on the cross-validation absolute error values of each sample for each oxide. The samples with the highest cross-validation absolute errors among the rest are removed from the data set. After outlier detection, PLS models are reconstructed with the remaining samples. The final PLS model was selected based on the model with the smallest SEP and the highest R^2 with an appropriate number of latent variables (LVs). Figure 2 depicts correlation graphs for major oxides, whereas Figure 3 depicts correlation graphs for minor oxides.

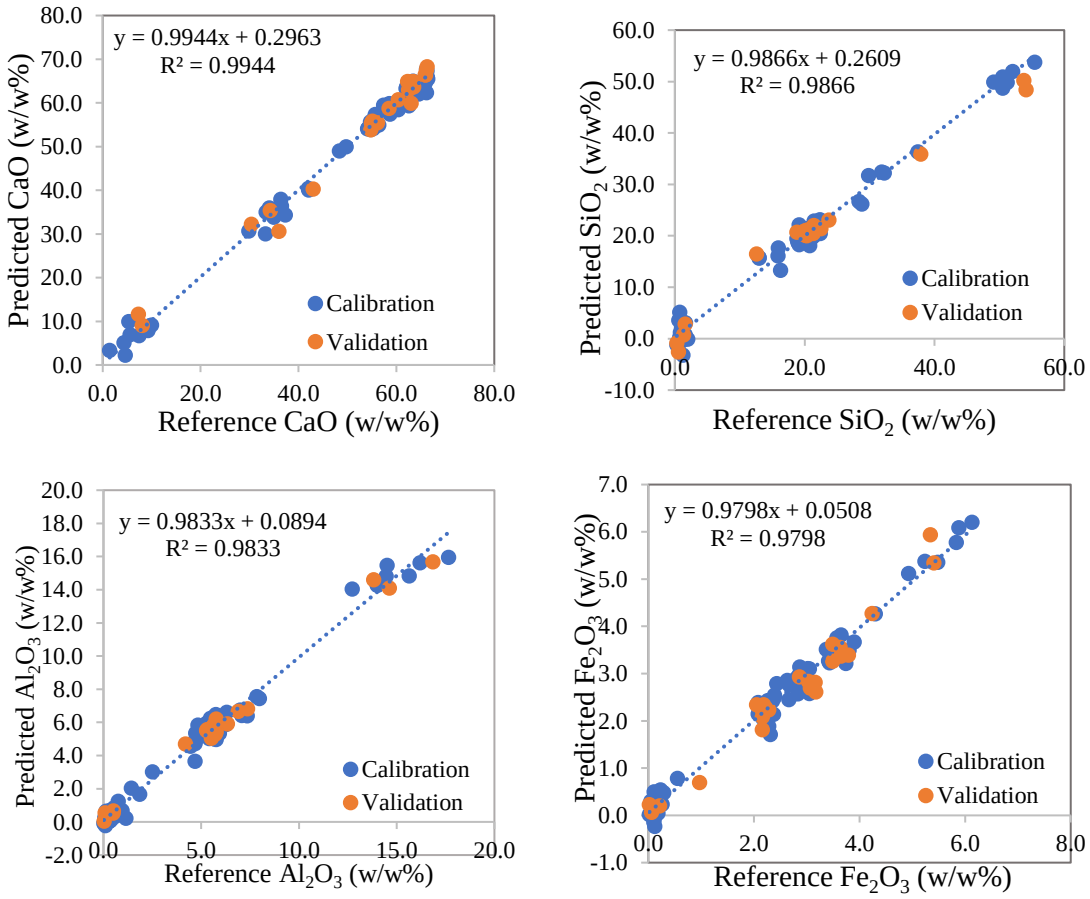

Figure 2. Reference versus predicted plots of PLS models constructed with EMSC applied FTIR-ATR spectra for CaO, SiO_2, Al_2O_3, Fe_2O_3

For the prediction of CaO concentration (w/w%), the first 10 latent variables (LVs) were incorporated into the PLS model. As shown in Figure 1, the correlation plot of CaO, the model performance of calibration, and the validation set predictions are quite similar, indicating no overfitting issue. In addition, the SECV and SEP values were determined to be 1.319% and 2.075% (w/w%), respectively. The calibration set's R^2 is calculated to be 0.994, while the validation set's R^2 is 0.987. After data mean-centering for SiO_2 concentration prediction, 6 LVs were chosen. The calibration (R^2) was found to be 0.986, while the predictive power of the validation data set (R^2) was 0.984. The model's performance for calibration and validation set predictions is very similar. In addition, the SECV and SEP values were calculated to be 1.416% and 1.96 %, respectively. For the PLS model of Al_2O_3, the R^2 values for the calibration and validation sets were 0.983 and 0.99, respectively. The SECV was calculated to be 0.486 (w/w%), while the SEP was calculated to be 0.455 (w/w%). The SEP value was lower than the SECV value, indicating a slight overfitting concern in the PLS model, but not a significant one because the regression coefficient quantities are close. For Fe_2O_3 concentration prediction, the R^2 values were found to be 0.978 and 0.968 of the calibration and validation, respectively. These results indicate that the model's

performance in predicting Fe_2O_3 concentrations in the validation samples is excellent because the calibration and validation correlations with reference XRF measurements are almost equal. The computed SECV and SEP values were 0.205 and 0.273 (w/w%), respectively. Despite the small concentration range of the samples, the Fe_2O_3 model demonstrated excellent prediction ability for the validation sample. It is important to note that the PLS regression models for the high-correlation main components (CaO, SiO_2, Al_2O_3, and Fe_2O_3) performed quite well.

Compared to a previously published related study, the present study reveals that the regression coefficients of the PLS models are greater for the major oxides. Especially considering the Fe_2O_3, the current study exhibits a remarkably higher PLS regression coefficient and comparable standard error of prediction (R^2: 0.98, SEP: 0.27 (w/w%)) than the previously published study (R^2: 0.63, RMSE: 0.22 (m/m%)) [16]. Also, PLS results are compared with another previously published study [17]. It can be said that regression coefficients of current PLS models for the major oxides are relatively higher than tose given in the literature, but the standard error of prediction (SEP) values are much higher than the values given at the same reference. One possible reason for this could be the diversity of the type of the materials used in our study whereas the literature values are given only for cement [16] and raw materials [17] but not for the combination of these materials together.

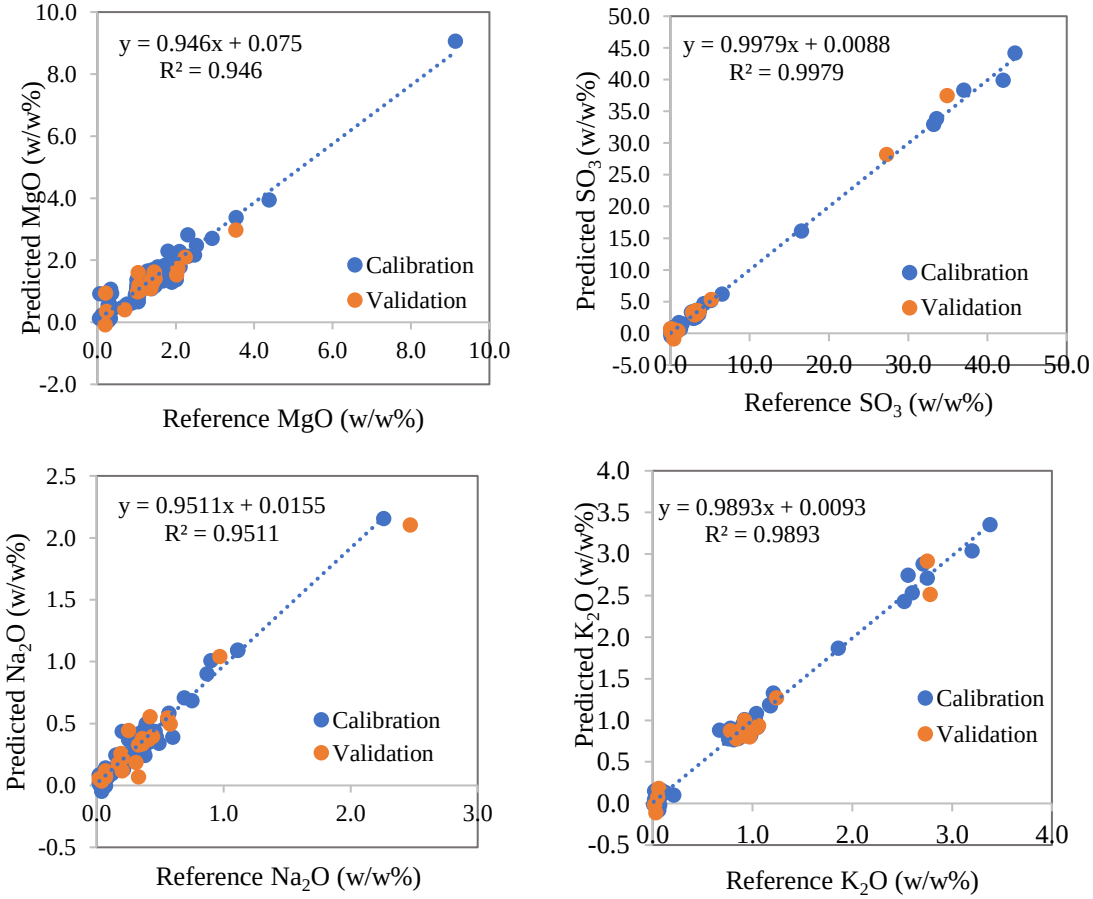

Figure 3. Reference versus predicted plots of PLS models constructed with EMSC applied FTIR-ATR spectra for MgO, SO_3, Na_2O, K_2O

For minor oxides also PLS models are constructed with appropriate number of LVs to predict their concentration in samples. For MgO, the PLS model for calibration and validation R^2 were found to be 0.94 and 0.89, respectively along with SECV and SEP values were 0.26% and 0.42% (w/w%). A close examination of reference XRF vs PLS predicted MgO plot reveals that calibration samples more scattered yet resulting in a lower SECV value compared to SEP value of independent validation samples. However, the number of calibration set samples are more than three times of validation set samples and there are

quite large number of samples in the calibration set which have much lower deviation from reference XRF values resulting in a lower SECV due to the averaging effect. When the PLS model for MgO was compared with the earlier published study, it can be sait that similar values are observed in terms of R^2 and SEP values (0.92 and 0.3 w/w%, respectively) [16]. For SO_3, the R^2 of the model was found to be 0.99 for the calibration set and 0.99 for the validation set along with quite low SECV and SEP values (0.39 and 0.68 w/w%, respectively) when compared to the dynamic range of the parameter which ranges from 0 to 45 w/w%. When the PLS model for SO_3 was compared with the another related study, R^2 and SEP values of the previous study were found to be 0.83 and 0.24 (w/w%), respectively [16]. For Na_2O, the R^2 values for the calibration and validation sets were 0.95 and 0.95, respectively, while the SECV and SEP values were computed to be 0.067 and 0.118 (w/w%), respectively. Despite the low Na_2O concentration in the samples, the model has strong predictive potential because of its excellent correlation with the reference analysis. For K_2O, the R^2 values for calibration and validation sets were 0.98 and 0.97, respectively. The computed SECV and SEP values were 0.072 and 0.104 (w/w%), respectively. Despite the restricted concentration range, the model's prediction ability is reasonably strong, indicating that the developed PLS model is robust. Although the PLS models performed well in terms of prediction for minor oxides, the regression coefficients were found lower when compared to major oxides. It can also be explained by the precision with which the reference measurement analysis for these oxides is measured. If the concentration values are not introduced correctly into the model, the PLS model may not be able to extract the correct concentration information from the spectra. Due to the "shadow effect," in which larger particles mask the X-ray signal emitted by smaller grains at the pellet's surface, bigger particle sizes at the sample's analysis surface might lead to errors. Elements, Na has a shallower escape depth than Fe, which has a shorter wavelength. Therefore, Na analysis is particularly sensitive to sample heterogeneities on this scale because it only samples the top 10 μm or so of a sample [27].

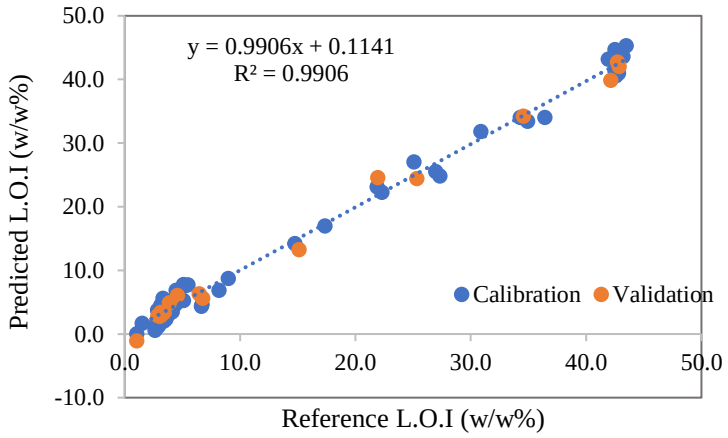

Figure 4. Reference versus predicted plots of PLS models constructed with EMSC applied FTIR-ATR spectra for loss of ignition (LOI)

For LOI, the calibration and validation set yielded R^2 of 0.99 and 0.99 for the model. The computed SECV and SEP values are 1.40 and 1.24 (w/w%), respectively. As can be seen from the plot, the dynamic range of the LOI model is comparable with SO_3 model and yet their R^2 values are very close to each other but when SECV and SEP values of the SO_3 and LOI models are compared the values for LOI model are much higher (0.39 and 0.68 w/w% for SO_3). The reason for these large difference may be explained with the shape of the reference vs predicted plot of LOI in which a large group of LOI values located between 3 to 7 w/w% and the second largest group of values around 43 w/w%. On the other hand, relatively small number of calibration samples are located in between 10 to 40 w/w% LOI. As a result, PLS model is mainly weighted from the two extreme ends and therefore fitting a reasonably good line for these two regions. Table 1 shows the statistical evaluation of the all parameters modeled in this study including the terms such as number of latent variables, SECV, SEP, R^2, maxium, minimum and dynamic range.

Table 1. SECV, SEP, and R^2 of CaO, SiO_2, Al_2O_3, Fe_3O_4, MgO, Na_2O, K_2O, and L.O.I models obtained with PLS along with number of latent variables (LVs), maximum, minimum concentrations (w/w%) of each parameter

	Latent Variables	**SECV (w/w%)**	**SEP (w/w%)**	**R^2**	**Max**	**Min**	**Range**
CaO	10	1.39	2.07	0.99	66.38	1.41	64.97
SiO2	6	1.42	1.97	0.99	55.42	0.28	55.14
Al_2O_3	11	0.49	0.45	0.98	17.66	0.02	17.64
Fe_2O_3	10	0.21	0.27	0.98	6.13	0.02	6.11
MgO	18	0.26	0.42	0.95	9.13	0.05	9.08
SO_3	13	0.40	0.69	0.99	43.48	0.05	43.43
Na_2O	13	0.07	0.12	0.95	2.26	0.02	2.24
K_2O	9	0.07	0.10	0.99	3.38	0.01	3.37
L.O.I	8	1.41	1.25	0.99	43.48	1.03	42.45

As can be seen from Table 1, the largest LVs is18 for MgO model whereas the smallest number of LVs is 6 for SiO_2.The rest of the LVs is ranged in between 8 to 10. It must be stated that the PLS models were constructed with EMSC pretreated FTIR-ATR spectra, therefore one may expect relatively smaller number of LVs for this pretreated spectral data, however, calibration data set is constructed not only with various types of cements but also a number of different additives and raw materials making the spectral data set quite complicated. In summary, the PLS regression models showed well performance, and the models may be used in cement facilities for fast screening of the raw materials and finished products.

Table 2. Comparison of the 95% reproducibility statics for the cement samples used in the independent validation set with respect to SEP values obtained from PLS models based on FTIR-ATR spectra.

Cement	**Mean(w/w%)**	**Min. (w/w%)**	**Max. (w/w%)**	**s_R**	**R**	**SEP(w/w%)**
CaO	59.71	54.68	64.74	0.24	0.67	0.62
SiO_2	21.57	18.51	24.63	0.19	0.53	0.81
Al_2O_3	5.47	4.54	6.40	0.19	0.53	0.37
Fe_2O_3	2.82	2.28	3.36	0.17	0.48	0.39
MgO	1.87	1.51	2.24	0.14	0.39	0.12
SO_3	2.10	0.96	3.25	0.17	0.48	0.21
Na_2O	0.44	0.22	0.66	0.09	0.25	0.05
K_2O	0.87	0.76	0.98	0.07	0.20	0.09
L.O.I	3.52	0.97	5.70	0.13	0.36	0.22

s_R: Reproducibility standard deviation. R: 95% reproducibility statics ($R = 2.8 \times s_R$)

In order to compare XRF reference method and FTIR-ATR in terms of uncertainty evaluation, 95% reproducibility statics for all types of cements, raw materials and additives were calculated in accordance with literature [10] and with Laboratory Test Programme (LTP) samples which are gathered from the Turkish Cement Manufacturers' Association and analyzed by many laboratories affiliated with the institution. Table 2 gives the 95% reproducibility statics of XRF reference analysis for the cement samples used in the independent validation set with respect to SEP values obtained from PLS models based on FTIR-ATR spectra. A detailed 95% reproducibility statics of XRF reference analysis for rest of the matrials used in this study is given in supporting templete as Table S3. (See supporting information) As can be seen from these tables, reproducibility standard deviation (s_R) values for XRF reference method are generally lower than the SEP values of PLS models obtained with FTIR-ATR

spectra. On the other hand, 95% reproducibility statics (R) computed for XRF method are comparable with the SEP values of PLS models. These result are also supported with a literature study [16] in which near infrared emission spectroscopy is used for rapid compositional analysis of Portland cements. Finally, to compare the developed FTIR-ATR based PLS method with the XRF standard reference method and evaluate its performance, paired t-test method was performed. Table 3 shows the results of the paired t-test at 95% confidence level for the concentrations of each oxide along with loose of ignition parameter obtained from XRF and FTIR-ATR based PLS models for the validation set.

Table 3. The results of the paired t-test for the concentrations of each oxide along with loose of ignition parameter obtained from XRF and FTIR-ATR based PLS models for the validation set.

	Mean	**Variance**	**t–calculated**	**p–value**	**t–table (two tail)**
Reference CaO	51.86	320.44	–0.90	0.38	2.08
Predicted CaO	52.25	315.99			
Reference SiO_2	20.73	188.74	1.04	0.31	2.07
Predicted SiO_2	20.31	164.44			
Reference Al_2O_3	6.02	17.86	1.09	0.29	2.07
Predicted Al_2O_3	5.92	16.53			
Reference Fe_2O_3	2.72	2.12	1.30	0.21	2.07
Predicted Fe_2O_3	2.65	2.18			
Reference MgO	1.47	1.08	–0.09	0.93	2.07
Predicted MgO	1.48	1.51			
Reference SO_3	4.32	71.84	–1.36	0.19	2.07
Predicted SO_3	4.50	80.86			
Reference Na_2O	0.41	0.25	0.74	0.47	2.07
Predicted Na_2O	0.39	0.19			
Reference K_2O	0.93	0.46	1.34	0.19	2.07
Predicted K_2O	0.90	0.45			
Reference L.O.I	14.77	249.27	0.87	0.40	2.11
Predicted L.O.I	14.52	242.80			

As shown in Table 3, all t-values generated by the t-test at 95% confidence level are less than the critical t-values. Consequently, it is fair to conclude that FTIR-ATR based PLS multivariate calibration may be used as a fast screening method in cement industry for the raw materials and finished products.

4. Conclusions

As an alternative to the current XRF approach, the present work has proven an analytical method for the quantitative determination of composition for cement raw materials, intermediate products, additives, and final products utilizing FTIR-ATR coupled with the chemometrics calibration method. The newly proposed approach is significantly faster than XRF because there is no need for additional sample preparation procedures. In addition, because XRF employs radioactive sources, the newly developed method is far safer. Furthermore, the new method has a lower instrumentation cost than other techniques. The study involves a variety of samples ranging from raw materials to finished cement products to estimate main and minor oxides and ignition loss. The higher-quality PLS models were created by applying extended multiplicative scatter correction (EMSC) thanks to the scattering reduction in the spectra caused by the sample particle size, and useful information is preserved. The present study showed that the regression coefficients (R^2) of the PLS models ranged from 0.95 to 0.99, whereas the SEP values ranged from 0.10 to 2.07 (w/w%). In addition, the paired t-test at a confidence level of 95% indicated that the analytical results produced by FTIR-ATR in association with PLS are similar to XRF measurements for all oxides examined. The predicted values could be used to track the cement manufacturing process and final composition. The robustness of PLS models could be enhanced by increasing the number of samples for each type.

Acknowledgements

The authors would like to thank BATIÇİM Batı Anadolu Cement Industry Co. Ltd. for providing XRF reference measurements and samples. This study is the part of MSc thesis of Dilek TEPELİ.

Supporting Information

Supporting information accompanies this paper on http://www.acgpubs.org/journal/ journal-of-chemical-metrology

ORCID
Dilek Tepeli: 0000-0002-5347-7254
Durmuş Özdemir: 0000-0003-3297-8217
Mehmet Gökhan Gümüş : 0000-0002-6536-613X

References

[1] Turkish Standard Institute (2008). TS EN 197-1. Cement–part 1: composition, specifications and conformity criteria for common cements.
[2] ASTM C114-15, Standard Test Methods for Chemical Analysis of Hydraulic Cement, ASTM Int, 2015, pp. 1e32,
[3] M.S. Ali, I. A. Khan and M.I. Hossain, (2008). Chemical analysis of ordinary Portland cement of Bangladesh, *Chem. Eng. Res. Bull*. **12**, 7-10.
[4] K.K. Choi, L. Lam and S.F. Luk (1994). Analysis of cement by atomic absorption spectrophotometry and volumetric method, *Talanta* **41(1),** 1–8.
[5] L. Capacho-Delgado and D. C. Manning (1967). The determination by atomic-absorption spectroscopy of several elements, including silicon, aluminium and titanium, in cement, *Analyst* **92**(**1098**), 553-557.
[6] L. Marjanovic, R. I. McCrindle, B.M. Botha and J. H. Potgieter (2000). Analysis of cement by inductively coupled plasma optical emission spectrometry using slurry nebulization, *J. Anal. At. Spectrom.* **15**(**8**), 983-985.
[7] C. S. Silva, T. Blanco and J. A. Nóbrega (2002). Analysis of cement slurries by inductively coupled plasma optical emission spectrometry with axial viewing, *Spectrochim. Acta B: At. Spectrosc*. **57**(**1**), 29-33.
[8] S. Khelifi, F. Ayari, H. Tiss and D. B. Hassan Chehimi (2017). X-ray fluorescence analysis of Portland cement and clinker for major and trace elements: accuracy and precision, *J. Aust. Ceram. Soc.* **53**(**2**), 743-749.
[9] M. A. Elbagermia, A. I. Alajtala and M. Alkerzab (2014). Chemical analysis of available Portland cement in libyan market using X-Ray Fluorescence, *Int. J. Chem., Mol., Nucl., Mat. Metall. Eng.* **8**(**1**), 73-75.
[10] P. Stutzman and A. Heckert (2014). Performance Criteria for Chemical Analysis of Hydraulic Cements by X-Ray Fluorescence Analysis Official contribution of the National Institute of Standards and Technology; not subject to copyright in the United States, *Adv. Civ. Eng. Mater*. **3**(**1**), 434-453.
[11] G. Walenta and T. Füllmann (2004). Advances in quantitative XRD analysis for clinker, cements, and cementitious additions, *Powder Diffr*. **19**(**1**), 40-44.
[12] ASTM, C. (2006). 1365-06. Standard Test Method for Determination of the Proportion of Phases in Portland Cement and Portland-Cement Clinker Using X-Ray Powder Diffraction Analysis, West Conshohocken, Pennsylvania: American Society of Testing Materials.
[13] TSI. (2002). TS EN 196-2: Methods of testing cement. Part 2: Chemical analysis of cement.
[14] N. Zaini, F. Van der Meer, F. Van Ruitenbeek, B. De Smeth, F. Amri and C. Lievens (2016). An alternative quality control technique for mineral chemistry analysis of Portland cement-grade limestone using shortwave infrared spectroscopy, *Remote Sens*. **8**(**11**), 950.
[15] S. Nasrazadani and T. Springfield (2014). Application of Fourier transform infrared spectroscopy in cement Alkali quantification, *Mater. Struct.* **47**(**10**), 1607-1615.
[16] J. P. Rebouças, J. J. R. Rohwedder and C. Pasquini (2018). Near infrared emission spectroscopy for rapid compositional analysis of Portland cements, *Anal. Chim. Acta*. **1024,** 136-144.
[17] Z. Yang, H. Xiao, L. Zhang, D. Feng, F. Zhang, M. Jiang and L. Jia (2020). Fast determination of oxides content in cement raw meal using NIR spectroscopy combined with synergy interval partial least square and different preprocessing methods, *Measurement* **149,** 106990.
[18] B. Yılmaz (2005). The comparative methods powder and glass done by XRF determine of main oxide components in cement clinker, *Dumlupınar Üniv. Fen Bilim. Enst. Derg*. **9**, 157-163.
[19] X.L. Cao, W. Zhao, R. Churchill and C. Hilts (2014). Occurrence of di-(2-ethylheyxyl) adipate and phthalate plasticizers in samples of meat, fish, and cheese and their packaging films, *J. Food Prot*. **77,** 610-620.
[20] J. Peng, S. Peng, Q. Xie and J. Wei (2011). Baseline correction combined partial least squares algorithm and its application in on-line Fourier transform infrared quantitative analysis, *Anal. Chim. Acta*. **690**(**2**), 162-168.

[21] H. Martens, J. P. Nielsen and S. B. Engelsen (2003). Light scattering and light absorbance separated by extended multiplicative signal correction. Application to near-infrared transmission analysis of powder mixtures, *Anal. Chem.* **75**(**3**), 394-404

[22] N.B. Gallagher (2006). Extended Multiplicative Scatter Correction Applied to Mid-Infrared Reflectance Measurements of Soil. Eigenvector. http://www. eigenvector. com/getwhitepaper. php.

[23] D. M. Haaland and E.V. Thomas (1988). Partial least-squares methods for spectral analyses. 1. Relation to other quantitative calibration methods and the extraction of qualitative information, *Anal. Chem.* **60**(**11**), 1193-1202.

[24] P. Geladi and B. R. Kowalski (1986). Partial least-squares regression: a tutorial, *Anal. Chim. Acta*. **185,** 1-17.

[25] T.T. Wong (2015). Performance evaluation of classification algorithms by k-fold and leave-one-out cross validation, *Pattern Recognit.* **48**(**9**), 2839-2846.

[26] T. L. Hughes, C. M. Methven, T. G. Jones, S. E. Pelham, P. Fletcher and C. Hall (1995). Determining cement composition by Fourier transform infrared spectroscopy, *Adv. Cem. Based Mater*. **2**(**3**), 91-104.

[27] D. Coler, L. Bruzenak, I. Campbell and C. Republic (2015). The common sources of error in sample preparation for XRF analysis and the capabilities of standalone automation (available from the corresponding author as a pdf file).